



Dynamics in a Respiratory Control Model With Two Delays

^{1*}Saroj P. Pradhan, ²Ferenc Hartung & ³Janos Turi

¹Department of Mathematics
Prairie View A& M University
Prairie View, TX 77446, USA
sppradhan@pvamu.edu

²Department of Mathematics
University of Pannonia
Veszprém, H-8201, Hungary
hartung.ferenc@uni-pannon.h

³Department of Mathematical Sciences
University of Texas at Dallas
Richardson, TX 75080, USA
turi@utdallas.edu

*Corresponding Author

Received: August 1, 2019; Accepted: October 4, 2019

Abstract

In this paper we study ventilation patterns in a set of parameter dependent nonlinear delay equations with two transport delays modeling the human respiratory control system with peripheral and central control loops. We present a convergent numerical scheme suitable to perform simulations when all disturbances and system parameters are known, then we consider the numerical identifiability of various system parameters based on ventilation data. We are especially interested in the identification of the transport delays in the control loops because these parameters are not measurable directly, but they have a strong influence on system stability/instability.

Keywords: Chemical balance dynamics; Respiratory control, Peripheral and central control loops, Multiple transport delays

MSC 2010 No.: Primary: 92B99, 34K20; Secondary: 93B52

1. Introduction

A simplified model of the human respiratory control system is formulated as a set of nonlinear, parameter dependent, delay differential equations with two transport delays (Eugene (2006), Pradhan and Turi (2013, 2016), Pradhan (2010)). System parameters determine the location and stability of the unique equilibrium in the model (see Pradhan and Turi (2013, 2016), Pradhan (2010) for details). Biological parameters change from person to person, they are also dependent on time, on sleep (including different sleep stages) or awakening, the physical condition of the individual, and possibly on other factors. Some of the parameters, and parameter changes are difficult and/or inconvenient to monitor, and therefore the availability of (on- or offline) parameter identification can play an important role in the study of regular and irregular ventilation patterns.

An important fact for our study is that many individuals diagnosed with sleep apnea are wearing CPAP masks during sleep, and consequently their ventilation data can be recorded and used for identification purposes. Of course, CPAP masks can leak, and thus the resulting ventilation data can become "noisy" making the identification process more challenging. Another issue is the identifiability of parameters using (noisy or not) ventilation data. In this paper, similarly to the study in Hartung and Turi (2013), we consider time segments of "information rich" ventilation data, i.e., instances when the system is forced to make transitions from one equilibrium point to a different one (due to changes in system parameters) and/or when it is forced to respond to an apneic event (obstructive or central) and establish "numerically observed identifiability" of system parameters.

Our main focus is to investigate the effects due to changes in the transport delays. Note that the transport delays are system parameters which don't influence the location of the unique equilibrium of the system but they can change the stability/instability of it. A strong motivation for the identification of transport delays comes from the observation that cardiac events (like congestive heart failure) can result in a significant change (increase) in their values leading to respiratory irregularities.

In Section 2 we describe the respiratory control model considered in this paper, in Section 3 we provide a short discussion on the numerical tools used to run simulations on the model equations and to construct stability charts (in terms of the transport delays) for given equilibrium points. Section 4 outlines the parameter identification process and includes case studies with main focus on the identification of transport delays and their effects on system behavior. Section 5 contains a discussion on our findings.

2. Respiratory Control Model

An overview of the respiratory control system is shown in Figure 1. It is based on two compartments (lung and brain) for blood gas exchange and storage. The model equations are balance equations for CO_2 and O_2 concentrations in the lung compartment and for CO_2 concentration in the brain compartment. We consider a system of nonlinear delay differential equations (see also Pradhan and Turi (2013)) describing a simple model of the human respiratory control system:

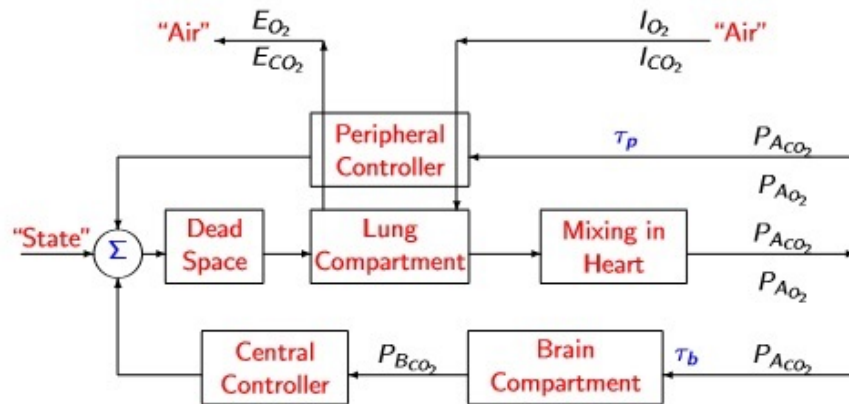


Figure 1. Block Diagram of the Respiratory Control System

$$\dot{x}_1(t) = a_{11} - a_{12}x_1(t) - a_{13}V(t, x_1(t - \tau_p), x_2(t - \tau_p), x_3(t))(x_1(t) - P_{I_{CO_2}}) \quad (1)$$

$$\dot{x}_2(t) = -a_{21} - a_{22}x_2(t) + a_{23}V(t, x_1(t - \tau_p), x_2(t - \tau_p), x_3(t))(P_{I_{O_2}} - x_2(t)) \quad (2)$$

$$\dot{x}_3(t) = a_{31} + a_{32}(x_1(t - \tau_b) - x_3(t)) \quad (3)$$

where $x_1(t)$, $x_2(t)$, and $x_3(t)$ represents arterial CO_2 , O_2 of the lung, and CO_2 concentrations of the brain, respectively, V is the ventilation function, τ_p is the transport delay from the lung to the carotid body, τ_b is the transport delay from the lung to the brain, and the coefficients a_{ij} are given as

$$a_{11} = 863 \frac{\dot{Q}K_{CO_2}P_{VCO_2}}{V_{ACO_2}}, \quad a_{12} = 863 \frac{\dot{Q}K_{CO_2}}{V_{ACO_2}}, \quad a_{13} = \frac{E_F}{V_{ACO_2}},$$

$$a_{21} = 863 \frac{\dot{Q}}{V_{AO_2}}(-M_V P_{VO_2} + B_A - B_V), \quad a_{22} = 863 \frac{\dot{Q}M_A}{V_{AO_2}}, \quad a_{23} = \frac{E_F}{V_{AO_2}},$$

$$a_{31} = \frac{MR_{BCO_2}}{M_{BCO_2}K_{BCO_2}}, \quad \text{and } a_{32} = \frac{\dot{Q}_B}{M_{BCO_2}}.$$

See also Table 1 for the names of the quantities appearing in a_{ij} .

It is assumed that the ventilation function has the form

$$V(t) = G_P(t)exp(-0.05(x_2(t - \tau_p))(x_1(t - \tau_p) - I_P)^+ + G_C(t)(x_3(t) - I_C)^+, \quad (4)$$

where the notation x^+ is defined as

$$x^+ = \begin{cases} x, & \text{if } x \geq 0, \\ 0, & \text{otherwise.} \end{cases}$$

For simplicity we assume that G_P and G_C are piecewise constant functions in time, and in particular,

$$G_P(t) = \begin{cases} G_{P1}, & 0 \leq t < \theta_1, \\ G_{P2}, & \theta_1 \leq t, \end{cases} \quad (5)$$

$$G_C(t) = \begin{cases} G_{C1}, & 0 \leq t < \theta_2, \\ G_{C2}, & \theta_2 \leq t. \end{cases} \quad (6)$$

We refer to the first and second terms in V as the peripheral and central ventilation functions, V_P and V_C , respectively. Peripheral and central ventilation correspond two control loops with different transport delays (i.e., τ_p and τ_b , respectively).

Table 1. Normal parameter values

| Name | Symbol | Unit | Value |
|--|----------------|-------------|---------|
| Peripheral Control Gain | G_P | l/min/mm Hg | 45 |
| Central Control Gain | G_C | l/min/mmHg | 1.2 |
| Rate of Blood Flow to the Brain | \dot{Q}_B | l/min | .75 |
| Cardiac Output | \dot{Q} | l/min | 6.0 |
| Oxygen (O_2) Concentration in air | $P_{I_{O_2}}$ | mmHg | 115.17 |
| Carbon Dioxide (CO_2) in air | $P_{I_{CO_2}}$ | mmHg | 0.22 |
| Dissociation Constant for CO_2 at the artery | K_{CO_2} | | .0057 |
| Dissociation Constant for CO_2 at the brain | K_{BCO_2} | | .0065 |
| Partial pressure of CO_2 in venous blood | $P_{V_{CO_2}}$ | mmHg | 46.0 |
| Partial pressure of O_2 in venous blood | $P_{V_{O_2}}$ | mmHg | 41.0 |
| Lung CO_2 volume | V_{ACO_2} | l | 3.2 |
| Lung O_2 volume | V_{AO_2} | l | 2.5 |
| Constant | M_V | | 0.0021 |
| Constant | M_A | | 0.00025 |
| Constant | B_V | | 0.0662 |
| Constant | B_A | | 0.1728 |
| Peripheral Apnic Threshold | I_P | mmHg | 35.0 |
| Central Apnic Threshold | I_C | mmHg | 35.0 |
| Dead Space Factor | E_F | | 0.7 |
| Metabolic production rate for CO_2 in the brain | MR_{BCO_2} | ml/min STPD | 0.042 |
| Metabolic production rate for CO_2 in the alveoli | MB_{CO_2} | l/min | 0.9 |
| Equilibrium Value of arterial CO_2 of the Lung | \bar{x}_1 | mm Hg | 39.0795 |
| Equilibrium Value of arterial O_2 of the Lung | \bar{x}_2 | mm Hg | 76.2070 |
| Equilibrium Value of CO_2 concentration of the Brain | \bar{x}_3 | mm Hg | 47.6949 |
| Equilibrium Value of Peripheral Ventilation | \bar{V}_P | | 3.4444 |
| Equilibrium Value of Central Ventilation | \bar{V}_C | | 4.0645 |

It is easy to see that the system described by equations (1) - (4) has a unique positive equilibrium, $(\bar{x}_1, \bar{x}_2, \bar{x}_3)$ for constant parameter values.

In particular, at equilibrium we have

$$0 = a_{11} - a_{12}\bar{x}_1 - a_{13}\bar{V}(\bar{x}_1 - P_{ICo_2}), \tag{7}$$

$$0 = -a_{21} - a_{22}\bar{x}_2 + a_{23}\bar{V}(P_{IO_2} - \bar{x}_2), \tag{8}$$

$$0 = a_{31} + a_{32}(\bar{x}_1 - \bar{x}_3), \tag{9}$$

and

$$\bar{V} = G_P \exp(-.05\bar{x}_2)(\bar{x}_1 - I_P)^+ + G_C(\bar{x}_3 - I_C)^+ \tag{10}$$

where \bar{V} is the equilibrium value of the ventilation.

From Equation (9) we obtain \bar{x}_3 in terms of \bar{x}_1 . Writing

$$\bar{V} = \frac{a_{11} - a_{12}\bar{x}_1}{a_{13}(\bar{x}_1 - P_{ICo_2})} = \frac{a_{21} + a_{22}\bar{x}_2}{a_{23}(P_{IO_2} - \bar{x}_2)}$$

using (7) and (8) we get \bar{x}_2 in terms of \bar{x}_1 . Substituting the expressions for \bar{x}_2 and \bar{x}_3 into (10), then (7) becomes a nonlinear equation for \bar{x}_1 with a unique positive solution.

Note that the unique positive equilibrium of system (1)-(4) depends on the parameters G_P, G_C, P_{ICo_2} , and P_{IO_2} , which means that a change in the values of those parameters forces the system to transit to the corresponding "new" equilibrium. During the transition process unstable respiratory patterns may arise which then can lead to further changes in parameter values (e.g., due to the resulting changes in sleep stages). The transport delays do not influence the location of the equilibrium, but can change its stability.

The local stability of the equilibrium of system (1)-(4) can be investigated using the linear variational system obtained by linearizing system (1)-(4) around the equilibrium. Let $X_i(t) = x_i(t) - \bar{x}_i$, $i = 1, 2, 3$, $\mathbf{X}(t) = (X_1(t), X_2(t), X_3(t))^T$, and $\bar{V}_{x_i} = V_{x_i}(\bar{x}_1, \bar{x}_2, \bar{x}_3)$, $i = 1, 2, 3$. Then the linear variational system for (1)-(4) is given by

$$\frac{d\mathbf{X}(t)}{dt} = A_0\mathbf{X}(t) + A_1\mathbf{X}(t - \tau_p) + A_2\mathbf{X}(t - \tau_b), \tag{11}$$

where

$$A_0 = \begin{pmatrix} -a_{12} - a_{13}\bar{V} & 0 & -a_{13}(\bar{x}_1 - P_{ICo_2})\bar{V}_{x_3} \\ 0 & -a_{22} - a_{23}\bar{V} & a_{23}(P_{IO_2} - \bar{x}_2)\bar{V}_{x_3} \\ 0 & 0 & -a_{32} \end{pmatrix},$$

$$A_1 = \begin{pmatrix} -a_{13}(\bar{x}_1 - P_{ICo_2})\bar{V}_{x_1} & -a_{13}(\bar{x}_1 - P_{ICo_2})\bar{V}_{x_2} & 0 \\ a_{23}(P_{IO_2} - \bar{x}_2)\bar{V}_{x_1} & a_{23}(P_{IO_2} - \bar{x}_2)\bar{V}_{x_2} & 0 \\ 0 & 0 & 0 \end{pmatrix}, \text{ and } A_2 = \begin{pmatrix} 0 & 0 & 0 \\ 0 & 0 & 0 \\ a_{32} & 0 & 0 \end{pmatrix}.$$

The associated characteristic equation is

$$\Delta(\lambda, \tau_p, \tau_b) = \det(\lambda I - A_0 - A_1 e^{-\lambda \tau_p} - A_2 e^{-\lambda \tau_b}) = 0. \tag{12}$$

For the computation of the roots of (12) the software TRACE-DDE (see Breda et al. (2009)) is used providing stability/instability information on the equilibrium of the nonlinear system as long as the rightmost eigenvalues are not located on the imaginary axis. In Figure 2, we display the stability chart (the shaded region is unstable) on the (τ_p, τ_b) plane for $\bar{X} = (39.0795, 76.2070, 47.6949)$ and $G_P = 45, G_C = 1.2, I_P = 35.0,$ and $I_C = 35.0$. For the simulation studies in the parameter estimation section we select reference points $A = (\tau_p = 24 \text{ sec}, \tau_b = 83 \text{ sec}), B = (\tau_p = 23 \text{ sec}, \tau_b = 59.1 \text{ sec}),$ and $C = (\tau_p = 22 \text{ sec}, \tau_b = 42 \text{ sec})$ outside, on the boundary, and inside of the stable region, respectively.

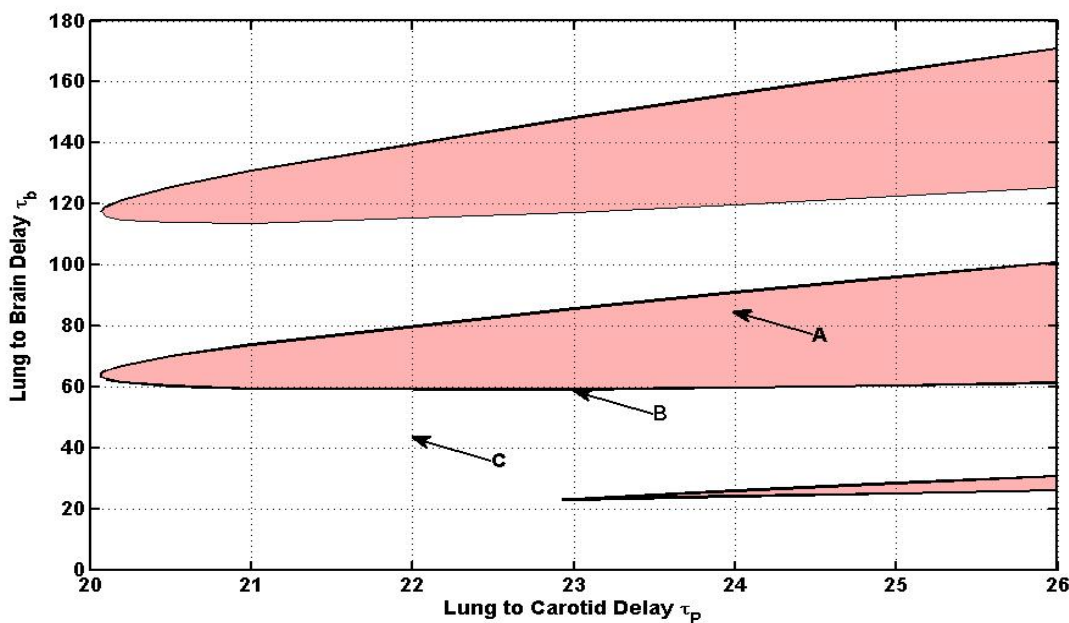


Figure 2. Stability Chart at $\bar{X} = (39.0795, 76.2070, 47.6949)$

3. Numerical Solutions of the Direct Problem

In this section we consider a simple numerical scheme based on approximation by delay differential equations with piecewise constant arguments (EPCAs) to approximate solutions of the system (1) – (4) assuming that all system parameters are known (direct problem).

Let h be a fixed positive constant, and define the notation $[t]_h = [\frac{t}{h}]h$, where $[\cdot]$ is the greatest integer function. Then $[t]_h$ as a function of t is piecewise constant, since $[t]_h = nh$ for $t \in [nh, (n + 1)h)$. For a fixed $h > 0$ we associate to (1)-(3) the discretized system (i.e., the EPCAs)

$$\begin{aligned} \dot{x}_{1_h}(t) &= a_{11} - a_{12}x_{1_h}([t]_h) - a_{13}V([t]_h, x_{1_h}([t]_h - [\tau]_h), \\ &\quad x_{2_h}([t]_h - [\tau]_h), \quad x_{3_h}([t]_h))(x_{1_h}([t]_h) - x_{1_l}), \end{aligned}$$

$$\begin{aligned}\dot{x}_{2_h}(t) &= -a_{21} - a_{22}x_{2_h}([t]_h) + a_{13}V([t]_h, x_{1_h}([t]_h - [\tau]_h), \\ &x_{2_h}([t]_h - [\tau]_h), x_{3_h}([t]_h))(-x_{2_h}([t]_h) + x_{2_I}),\end{aligned}$$

and

$$\dot{x}_{3_h}(t) = a_{31} + a_{32}x_{1_h}([t]_h) - a_{32}x_{3_h}([t]_h).$$

The solutions, $x_{1_h}(t)$, $x_{2_h}(t)$ and $x_{3_h}(t)$, $t \geq 0$, of the discretized system are continuous functions, which are differentiable and satisfy the discretized equations on each interval $(nh, (n+1)h)$ ($n = 0, 1, 2, \dots$). In particular, since the right-hand sides of the discretized equations are constant on each interval $[nh, (n+1)h)$, we get that $x_{1_h}(t)$, $x_{2_h}(t)$ and $x_{3_h}(t)$ are piecewise linear continuous functions (linear spline functions). Therefore, they are determined completely by their values at the mesh points nh .

We introduce the sequences $u_n = x_{1_h}(nh)$, $v_n = x_{2_h}(nh)$, and $w_n = x_{3_h}(nh)$ representing the mesh point values and let $k = \lceil \frac{\tau}{h} \rceil$.

Integrating then the discretized equations from nh to t and taking the limit as $t \rightarrow (n+1)h$, we get by simple calculations that u_n , v_n and w_n satisfy the system

$$u_{n+1} = u_n + h \left(a_{11} - a_{12}u_n - a_{13}V(nh, u_{n-k}, v_{n-k})(u_n - x_{1I}) \right), \quad (13)$$

$$v_{n+1} = v_n + h \left(-a_{21} - a_{22}v_n + a_{23}V(nh, u_{n-k}, v_{n-k})(x_{2I} - v_n) \right), \quad (14)$$

$$w_{n+1} = w_n + h \left(a_{31} + a_{32}u_n - a_{32}w_n \right), \quad (15)$$

for $n = 0, 1, 2, \dots$

For negative values, $n < 0$, the sequences u_n , v_n and w_n are defined by $u_n = x_{1_h}(nh)$, $v_n = x_{2_h}(nh)$, and $w_n = x_{3_h}(nh)$, i.e., using the initial functions corresponding to the original system (1)–(3). Therefore the sequences u_n , v_n and w_n are well-defined and can be easily generated by the explicit delayed recurrence relations (13)–(15), so piecewise linear approximations to the solutions of equations (1)–(3) are uniquely determined. It follows by Theorem 2.5 in Györi et al. (1995) that

$$\lim_{h \rightarrow 0^+} (x_{1_h}(t), x_{2_h}(t), x_{3_h}(t)) = (x_1(t), x_2(t), x_3(t)),$$

uniformly on each interval $[0, T]$, for any $T > 0$.

Note that the approximation process described above allows us to run simulations for the respiratory system as long as all system parameters are known (direct problem) as demonstrated next.

Example 3.1.

In this example we study numerically the effects of changing the values of the peripheral and central gains for the stability of the respiratory system (1)–(3). We assume normal table values

except we use $\tau_p = 19$ sec, and $\tau_c = 70$ sec, i.e., with ventilation (4)-(6). Furthermore, in (5) we select $\theta_1 = 10$ sec, and in (6) we select $\theta_2 = 30$ sec for the switching times, and $G_{P1} = 45$, $G_{P2} = 55$, $G_{C1} = 1.2$ and $G_{C2} = 1.8$ for the peripheral and central control gains. We start the system from its equilibrium corresponding to the $G_{P(t)} = G_{P1}$ and $G_{C(t)} = G_{C1}$ constant gains, i.e., use (constant) initial functions

$$x_1(t) = 39.0795, \quad x_2(t) = 76.2071, \quad \text{and} \quad x_3(t) = 47.6949, \quad \text{for } t \leq 0.$$

The numerical solution corresponding to discretization $h = .01$ is shown in Figure 3.

We can see from Figure 3: (i) for $0 \leq 10$ the equilibrium of the system with gains G_{P1} and G_{C1} is initially the triplet $(39.0795, 76.2070, 47.6949)$; (ii) it is forced to change at $t = 10$ to the triplet $(38.8956, 77.1665, 47.5109)$ and that "new" equilibrium is unstable for $10 \leq t \leq 30$ after switching the peripheral gain to G_{P2} ; (iii) the equilibrium is forced to change again at $t = 30$ to the triplet $(38.5888, 78.6841, 47.2041)$ and that "new-new" equilibrium is asymptotically stable for $t \geq 30$ after switching the central gain to G_{C2} .

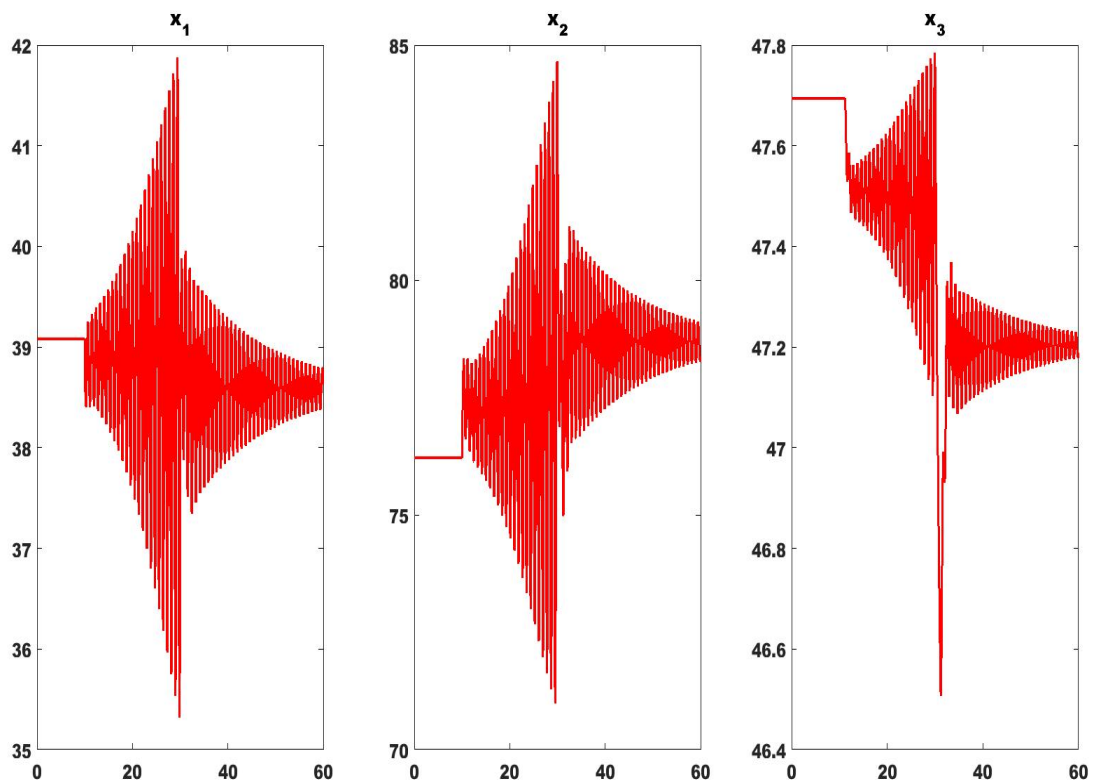


Figure 3. Effects of changing the control gains with switching times $\theta_1 = 10$ and $\theta_2 = 30$ and gain constants $G_{P1} = 45$, $G_{C1} = 1.2$, $G_{P2} = 55$, $G_{C2} = 1.8$

In the next section we attempt to find unknown, possibly time dependent, parameter values (inverse problem) using only ventilation data.

4. Parameter Estimation using Ventilation Data

We consider again system (1)–(3) with ventilation equation (4), assume that some parameters in this system are not known, and we denote these unknown parameters by an m -component vector, γ . The goal is to determine the values of these unknown parameters, assuming we know the measurements of the solutions at finitely many times, t_1, t_2, \dots, t_M . One standard approach to this problem is to minimize a least-square cost function, i.e., find the parameter values corresponding to the least possible cost.

We shall use the notations $x_1(t; \gamma)$, $x_2(t; \gamma)$, and $x_3(t; \gamma)$ to indicate solutions corresponding to the unknown parameters γ . Without loss of generality we assume equally spaced measurements over a time interval $[T_0, T]$, i.e.,

$$t_i = T_0 + \frac{T - T_0}{M}i, \quad i = 0, 1, \dots, M. \quad (16)$$

Then we define the cost function by

$$J(\gamma) = \sum_{i=0}^M (V(t_i, x_1(t_i; \gamma), x_2(t_i; \gamma), x_3(t_i; \gamma)) - V_i)^2,$$

where $V_i = V(t_i, x_1(t_i; \bar{\gamma}), x_2(t_i; \bar{\gamma}), x_3(t_i; \bar{\gamma}))$ with the "true" parameter value $\bar{\gamma}$.

Then the mathematical problem is to find γ which minimizes the cost function J . One standard approach to solve this problem, used, e.g., in Hartung et al. (1997, 1998, 2000) and Hartung and Turi (1997, 2000), is the following: find piecewise constant approximate solutions $x_1^N(t; \gamma)$, $x_2^N(t; \gamma)$, $x_3^N(t; \gamma)$ of equations (1)–(3), define

$$J^N(\gamma) = \sum_{i=1}^M (V(t_i, x_1^N(t_i; \gamma), x_2^N(t_i; \gamma), x_3^N(t_i; \gamma)) - V_i)^2,$$

and find the minimizer γ^N of J^N . One can show that, under minor assumptions, the sequence $\{\gamma^N\}_1^\infty$ (or more precisely, a subsequence of it) approaches the minimizer of J .

Next, we consider a sequence of h_N discretization constants converging to 0, and use the approximation scheme defined above in the corresponding computation. Then if N is large enough, i.e., equivalently, h_N is small enough, we find the minimizer of the corresponding cost function J^N by a nonlinear least square minimization code, based on a secant method with Dennis-Gay-Welsch update, combined with a trust region technique (see section 10.3 in Dennis and Schnabel (1998)). We know that the numerical method converges only locally, so we have to find a close enough initial guess of the parameters to observe convergence. Note that failure of convergence can also happen if we don't have identifiability of the parameters. On the other hand, convergence of the method indicates "numerical identifiability" as a by-product. We refer the reader to Lunel (2001) for a general discussion on identifiability of parameters in delay differential equations.

We will demonstrate the effectiveness of our parameter estimation procedure on the identification of the transport delays τ_p and τ_b . To put this experiment into proper perspective for the reader, we make a few observation beforehand:

(i) The system equilibrium is independent from the transport delays, and therefore if we start the system from its equilibrium, then changing the time delay has no effect on the solution. Therefore, it is not possible to identify the delays from the corresponding (constant) measurements.

(ii) Due to (i) it is necessary to force the system away from its equilibrium. To accomplish that we can use again the ventilation function defined by the parameters

$$\theta_1 = 10 \text{ sec}, \quad \theta_2 = 30 \text{ sec}, \quad G_{P1} = 45, \quad G_{P2} = 55, \quad G_{C1} = 1.2, \quad G_{C2} = 1.8.$$

(iii) We also observed that if we use measurements on the time interval where the solution is still constant, i.e., on $[0, 12 \text{ sec}]$, then at these points the solution does not depend on the delays, and the numerical minimization method will not usually converge. Therefore we used the interval $[T_0, T] = [18 \text{ sec}, 120 \text{ sec}]$ to make measurements using equidistant time points with $M = 10$.

(iv) In this experiment the convergence of the scheme is sensitive for the selection of the initial parameter value. The reason of it is that if at any step the numerical scheme produces a “large” τ_p or τ_b , then using that τ_p or τ_b the corresponding solution will be constant on the time interval $[18 \text{ sec}, 120 \text{ sec}]$, therefore the minimization will fail.

(v) Also, in identifying the delays the discretization constant has to be very small, since otherwise small changes in the delays will not effect the approximate solution, so the minimization will fail. For the same reason, in the minimization code the parameter which determines the time steps of computing approximate derivatives has to be relatively large otherwise again changes in the delays will not effect the solution, so the minimization will fail.

Example 4.1.

In this example, we assume that the equilibrium is $\bar{X} = (39.0797, 76.2070, 47.6949)$, the transport delays τ_p and τ_b are the unknown parameters and consider three cases (to be identified): $\tau_p = 22 \text{ sec}$, and $\tau_b = 42 \text{ sec}$ (point C in Figure (2)), $\tau_p = 23 \text{ sec}$, and $\tau_b = 59.1 \text{ sec}$ (point B in Figure (2)), and $\tau_p = 24 \text{ sec}$, and $\tau_b = 83 \text{ sec}$ (point A in Figure (2)).

Starting from \bar{X} , $\tau_p = 30 \text{ sec}$, and $\tau_b = 78 \text{ sec}$ in all three cases, applying the switching strategy described in (ii) (see also Example 3.1), and using $h = 0.00005$ we get convergent sequences for $x_1(t)$, $x_2(t)$, $x_3(t)$, and $V(t)$. In Table (2), Table (3), and Table (4) we show how the corresponding values of the cost function and the estimated values of the parameters τ_p and τ_b change from iteration to iteration. In all three cases the convergence is very fast and we get very good approximations of the “true” delay values in four or five iterations.

Table 2. Estimation of τ_p and τ_b at point C

| step | cost | τ_p | τ_b | $\Delta(\tau_p)$ | $\Delta(\tau_b)$ |
|------|----------|----------|----------|------------------|------------------|
| 0 | 72.01627 | 30.00000 | 78.00000 | 8.00000 | 36.00000 |
| 1 | 0.06005 | 21.71820 | 41.55240 | 0.28180 | 0.44760 |
| 2 | 0.00231 | 21.99300 | 41.92260 | 0.00700 | 0.07740 |
| 3 | 0.00000 | 22.00620 | 42.00018 | 0.00620 | 0.00018 |
| 4 | 0.00000 | 22.00620 | 41.99820 | 0.00620 | 0.00018 |

Table 3. Estimation of τ_p and τ_b at point B

| step | cost | τ_p | τ_b | $\Delta(\tau_p)$ | $\Delta(\tau_b)$ |
|------|----------|----------|----------|------------------|------------------|
| 0 | 11.67456 | 30.00000 | 78.00000 | 7.00000 | 18.90000 |
| 1 | 0.28932 | 23.69340 | 62.09100 | 0.69340 | 2.99100 |
| 2 | 0.00541 | 23.05860 | 59.52060 | 0.05860 | 0.42060 |
| 3 | 0.00060 | 23.02740 | 58.97700 | 0.02740 | 0.12300 |
| 4 | 0.00000 | 23.00580 | 59.10120 | 0.00580 | 0.00120 |
| 5 | 0.00000 | 23.00100 | 59.10120 | 0.00100 | 0.00120 |

Table 4. Estimation of τ_p and τ_b at point A

| step | cost | τ_p | τ_b | $\Delta(\tau_p)$ | $\Delta(\tau_b)$ |
|------|---------|----------|----------|------------------|------------------|
| 0 | 145.017 | 30.0000 | 78.0000 | 6.00000 | 5.00000 |
| 1 | 0.31080 | 23.74200 | 82.91100 | 0.25800 | 0.08900 |
| 2 | 0.01500 | 24.05820 | 83.01540 | 0.05820 | 0.01540 |
| 3 | 0.00060 | 24.01260 | 83.00220 | 0.01260 | 0.00220 |
| 4 | 0.00000 | 23.99940 | 82.99920 | 0.00060 | 0.00080 |
| 5 | 0.00000 | 24.00180 | 82.99920 | 0.00180 | 0.00080 |

5. Conclusion

It is assumed that ventilation measurements are available (which is the case for individuals wearing CPAP masks) for a simplified model of the respiratory control system. Based on a convergent approximation scheme, a parameter identification technique is applied then to determine system parameters as functions of time. It is an especially significant realization that using the available ventilation data changes in the transport delays can be identified.

REFERENCES

- Breda, D., Maset, S. and Vermiglio, R. (2009). TRACE-DDE: a Tool for Robust Analysis and Characteristic Equations for Delay Differential Equations, Topics in Time Delay Systems: Analysis, Algorithms, and Control, Lecture Notes in Control and Information Sciences, Vol. 388, pp. 145–155.
- Dennis, J.E. and Schnabel, R.B. (1998). *Numerical Methods for Unconstrained Optimization and Nonlinear Equations*, Prentice-Hall.
- Eugene, N.E. (2006). Why do we have both peripheral and central chemoreceptors?, Journal of Applied Physiology, Vol. 100, No. 1, pp. 9–10.
- Gyóri, I., Hartung, F. and Turi, J. (1995). Numerical approximations for a class of differential equations with time- and state-dependent delays, Applied Math. Letters, Vol. 8, Issue 6, pp. 19–24.
- Hartung, F., Herdman, T.L. and Turi, J. (1997). On existence, uniqueness and numerical approxi-

- mation for neutral equations with state-dependent delays, *Applied Numerical Mathematics*, Vol. 24, pp. 393–409.
- Hartung, F., Herdman, T.L. and Turi, J. (1998). Parameter identification in classes of hereditary systems of neutral type, *Appl. Math. Comput.*, Vol. 89, Issues 1-3, pp. 147–160.
- Hartung, F., Herdman, T.L. and Turi, J. (2000). Parameter identifications in classes of neutral differential equations with state-dependent delays, *Nonlinear Analysis: Theory, Methods & Applications*, Vol. 39, Issue 3, pp. 305–325.
- Hartung, F. and Turi, J. (1997). Identification of parameters in delay equations with state-dependent delays, *Nonlinear Analysis: Theory Methods & Applications*, Vol. 29, Issue 11, pp. 1303–1318.
- Hartung, F. and Turi, J. (2000). Linearized stability in functional differential equations with state dependent delays, *Discrete and Continuous Dynamical Systems (Added Volume)*, pp. 416–425.
- Hartung, F. and Turi, J. (2013). Parameter Identification in a Respiratory Control System Model with Delay. In *Mathematical Modeling and Validation in Physiology, Lecture Notes in Mathematics, Vol. 2064* (J.J. Batzel et al., Editors), pp. 105–118, Springer International Publishing.
- Lunel, S.M.V. (2001). Parameter identifiability of differential delay equations, *International Journal of Adaptive Control and Signal Process*, Vol. 15, pp 655–678.
- Pradhan, S.P. (2010). *The Role of Peripheral and Central Chemoreceptors in the Stability of the Human Respiratory System*, Ph.D. dissertation, University of Texas at Dallas.
- Pradhan, S.P. and Turi, J. (2013). Parameter dependent stability/instability in a human respiratory control system model, *Discrete and Continuous Dynamical Systems (Supplement 2013)*, pp. 631–640.
- Pradhan, S.P. and Turi, J. (2016). Effects of CPAP therapy on respiratory control system stability, *Dynamics of Continuous, Discrete and Impulsive Systems; Series B: Applications and Algorithms* Vol. 23, pp. 421–432.